THE SEVERE THUNDERSTORM ELECTRIFICATION AND PRECIPITATION STUDY

BY TIMOTHY J. LANG, L. JAY MILLER, MORRIS WEISMAN, STEVEN A. RUTLEDGE, LLYLE J. BARKER III, V. N. BRINGI, V. CHANDRASEKAR, ANDREW DETWILER, NOLAN DOESKEN, JOHN HELSDON, CHARLES KNIGHT, PAUL KREHBIEL, WALTER A. LYONS, DON MACGORMAN, ERIK RASMUSSEN, WILLIAM RISON, W. DAVID RUST, AND RONALD J. THOMAS

Data from a field project on the Colorado–Kansas border in summer 2000 is helping to improve our understanding of positive cloud-to-ground lightning and low-precipitation storms.

Severe thunderstorms, because of their propensity to injure, kill, and cause extensive property damage, are a primary concern to not only weather forecasters but also the public. However, these storms remain a puzzling scientific and forecasting problem, as they exhibit not only a wide range of electrical activity, but also diversity in precipitation type and amount. One of the more intriguing severe storms types in this regard is the supercell thunderstorm (Browning 1964). In its most pristine state, a supercell is a unicellular thunderstorm comprised of a single, long-lived, rotating updraft, and it frequently produces large hail, high winds, prolific lightning, and occasionally tornadoes. While the basic dynamics of supercells seem well understood (e.g., Klemp 1987), these storms exhibit a wide variety of precipitation characteristics that are not understood. For instance, supercells have been classified as either low precipitation (LP; Donaldson et al. 1965; Davies-Jones et al. 1976; Burgess and Davies-Jones 1979; Bluestein and Parks 1983), classic or medium precipitation (MP), or heavy precipitation (HP; Doswell and Burgess 1993; Rasmussen and Straka 1998) based on visual observations of the cloud and precipitation shafts. Perhaps the least-understood among these storms are LP supercells, which characteristically produce some large hail but little rain. Potentially because of the dry environment and lack of visible precipitation, the visible cloud below the anvil is a skeleton compared with

AFFILIATIONS: LANG, RUTLEDGE, BRINGI, AND CHANDRASEKAR—Colorado State University, Fort Collins, Colorado; MILLER, WEISMAN, AND KNIGHT—National Center for Atmospheric Research, Boulder, Colorado; BARKER—National Weather Service, Lincoln, Illinois; DETWILER AND HELSDON—South Dakota School of Mines and Technology, Rapid City, South Dakota; DOESKEN—Colorado Climate Center, Fort Collins, Colorado; KREHBIEL, RISON, AND THOMAS—New Mexico Institute of Mining and Technology, Socorro, New Mexico; LYONS—FMA Research, Inc., Fort Collins, Colorado; MACGORMAN, RASMUSSEN, AND RUST—National Severe Storms Laboratory, Norman, Oklahoma
CORRESPONDING AUTHOR: Timothy J. Lang, Department of Atmospheric Science, Colorado State University, Fort Collins, CO 80523
E-mail: tlang@atmos.colostate.edu
DOI: 10.1175/BAMS-85-8-1107

In final form 26 March 2004

other supercell storms (Bluestein and Parks 1983; Bluestein and Woodall 1990).

Another unusual aspect of some convective storms, including supercells, is their tendency to produce copious positive cloud-to-ground (+CG) lightning (e.g., Branick and Doswell 1992; Curran and Rust 1992; Carey and Rutledge 1998; Williams 2001), in contrast with most warm-season thunderstorms that produce predominantly negative CG lightning (~90% of all warm-season CGs are negative; Orville 1994; Orville and Silver 1997; Orville and Huffines 2001). In fact, the percentage of CG lightning that is positive in these storms [predominantly positive CG (PPCG) storms] can be far greater than 50%, sometimes approaching 100%. Many PPCG storms are severe, but not all severe storms are PPCG (Carey and Rutledge 2003; Carey et al. 2003), and we currently do not understand what exactly distinguishes PPCG storms from other storms.

Researchers typically observe two major positive charge regions within the updrafts of ordinary thunderstorms, an upper one (above the –20°C isotherm altitude; the main reservoir for positive charge) and a lower one (near 0°C altitude), with a major negative charge region (thought to be the source region for most –CGs) in between (i.e., between –10° and –20°C altitude; e.g., Krehbiel 1986; Koshak and Krider 1989; Stolzenburg et al. 1998a,b). This typical structure is often thought of as a dipole (main upper positive charge over midlevel negative) or tripole (considering the commonly observed lower positive charge; Williams 1989), although thunderstorm charge structures can be more complex than a simple dipole or tripole, particularly outside the main updraft (Stolzenburg 1998a,b). However, PPCG storms may not have typical electrical structures. Indeed, outstanding issues in +CG research include identifying the positive charge region that is the source for +CGs, and in addition, understanding if, how, and why the charge structures in PPCG storms differ from ordinary thunderstorms. Williams (2001) reviewed hypotheses for positive CG storms, and testing these hypotheses requires more information on relationships between precipitation formation, airflow kinematics, electrification, and lightning production in PPCG thunderstorms.

The ability to understand these relationships, however, requires sophisticated tools to observe and analyze thunderstorm characteristics. In particular, for precipitation, research with polarimetric radars has led to an emerging capability for identifying hydrometeor types remotely (Vivekandan et al. 1999; Liu and Chandrasekar 2000; Straka et al. 2000). Such work began with efforts to discriminate between hail and rain, but as these radars became more sophisticated, the number of observed variables and thus the number of potential discriminants increased. Some algorithms distinguish between such diverse hydrometeor types as large and small hail, graupel, snow, and mixed-phase precipitation. Hydrometeor identification can be useful in various applications to weather forecasting and aviation weather warnings, as well as in fundamental studies of storm structure and evolution. However, like all remote sensing techniques, polarimetric hydrometeor classification needs in situ verification to establish and improve the scope of its validity.

During May–July 2000, the Severe Thunderstorm Electrification and Precipitation Study (STEPS; Weisman and Miller 2000; http://box.mmm.ucar.edu/pdas/STEPS.html) took place near the Colorado–Kansas border in order to achieve a better understanding of the interactions between kinematics, precipitation production, and electrification in severe thunderstorms. Specific scientific objectives included 1) understanding the apparent major differences in precipitation output from supercells that have led to their being classified as LP, MP, and HP; 2) understanding lightning occurrence and behavior in storms, and how it differs among storm types, particularly to better understand the mechanisms by which storms produce predominantly +CG lightning; and 3) verifying and improving microphysical interpretations from polarimetric radar. Additionally, the emphasis on +CG lightning enabled research into what is different about the small subset of +CGs, usually from large thunderstorms known as mesoscale convective systems (MCSs), that trigger mesospheric transient luminous events (TLEs) such as sprites (Lyons et al. 2000, 2003a,b; Williams 1998). This latter problem has important implications for our understanding of how TLEs occur.

This paper is intended to be an overview of the STEPS field campaign and in addition provides a brief examination of STEPS research in order to demonstrate how the design and execution of the field campaign helped address the project goals. Because of length constraints, this paper mainly, though not exclusively, focuses on the positive CG issue (STEPS goal no. 2) in discussing the STEPS project.

STEPS DESIGN AND EXECUTION. The STEPS project brought together a unique suite of complementary observing platforms in eastern Colorado and western Kansas. The basic geographical layout of the project is shown in Fig. 1. This portion of the High Plains region of the United States has been

observed climatologically to favor supercell storms, particularly the LP variety (Bluestein and Parks 1983). This is primarily due to the warm-season presence in this region of the dryline, the boundary between moist air from the Gulf of Mexico and drier continental air, which has been strongly associated with the occurrence of LP storms. This association exists possibly because LP storms form in environments that are drier and have less low-level shear than traditional supercell environments, characteristics that drylines could provide via proximity to dry air, as well as enhanced mixing to reduce shear values (Bluestein and Parks 1983). However, little is understood about how exactly dryline proximity affects the kinematic and microphysical structure of LP storms. The STEPS region also is favorable for thunderstorms that produce predominantly +CG lightning (Zajac and Rutledge 2001; Carey and Rutledge 2003; Carey et al. 2003) as well as severe hailstorms (Changnon 1977). Thus, the STEPS domain was ideal for studying the storms of interest.

We specifically designed the field measurements and analysis for STEPS to explore the mechanisms of precipitation formation and lightning production in supercell and other storms. The instrumentation, listed in Table 1, included two S-band (~10 cm wavelength) polarimetric radars, the Colorado State University dual-polarization Doppler radar (CSU–CHILL) near Burlington, Colorado, and the National Center for Atmospheric Research (NCAR) S-band dual-polarization Doppler radar (S-Pol) near Idalia, Colorado, along with the S-band National Weather Service (NWS) Weather Surveillance Radar-1988 Doppler (WSR-88D) at Goodland, Kansas. Collectively, these radars determined the internal airflow and precipitation structure of storms. The CSU–CHILL and S-Pol radars are both dual-linearly polarized, providing information on the size, shape, orientation, and thermodynamic phase of hydrometeors. The network of three Doppler radars provided the opportunity to examine the three-dimensional inter-

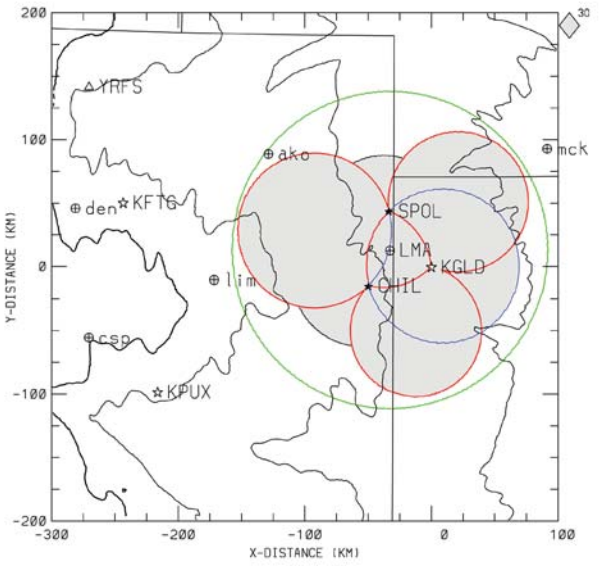

Fig. 1. Nominal areas of coverage (shading) by the triple-Doppler radar network. Outer dual-Doppler lobes (beam angles greater than 30°) and the inner triple-Doppler triangle are outlined in red. The second dual-Doppler lobe for the research radars CSU–CHILL (CHIL) and S-Pol (SPOL) is outlined in blue. The region within which vertical resolution is better than 1 km for the LMA is outlined in green (~125 km radius). Topographic height contours (black lines) are at 3, 4, 5, and 6 kft. NWS radars are shown for Denver, CO (KFTG), Pueblo, CO (KPUX), and Goodland, KS (KGLD), along with the Yucca Ridge Field Station (YRFS). Landmarks are shown at Denver (den), Colorado Springs (csp), Limon (lim), and Akron, CO (ako), and at McCook, NE (mck). All distances are east–west (*x*) and north–south (*y*) from the Goodland WSR-88D.

Table 1. List of STEPS instrumentation and their primary purposes during the project.

Platform	Purpose
Radar network	Characterize precipitation structure and airflow in thunderstorms
LMA	Map lightning discharges in three dimensions
NLDN	Locate ground strike locations and times of cloud-to-ground lightning
T-28 armored research aircraft	In situ observations of thunderstorm microphysics, electric fields, and winds
Balloon-borne EFM	In situ observations of electric fields, winds, and thermodynamics
Mobile mesonet	Characterize surface mesoscale environment of thunderstorm
M-GLASS soundings	Characterize thermodynamic structure and wind shear of environment
YRFS	Record observations of TLEs over thunderstorms

nal airflow of STEPS storms, via postproject synthesis of the multiple-Doppler observations.

The deployable Lightning Mapping Array (LMA) from the New Mexico Institute of Mining and Technology mapped the three-dimensional total lightning activity. The system located the sources of impulsive very high frequency (VHF) radio signals from the lightning by measuring the time that the signals arrived at the 13 receiving stations deployed over a 60–80-km-diameter area in northwestern Kansas and eastern Colorado. The LMA locates numerous VHF sources from the lightning activity, which can be grouped into individual flashes either manually using special analysis software or through an automated algorithm such as that of Thomas et al. (2003), by considering the spatial and temporal proximity of VHF sources to one another. The LMA is most sensitive to VHF radiation from negative breakdown occurring within regions of net positive charge (Mazur et al. 1997; Rison et al. 1999). Thus, the LMA can be used to identify major positive charge regions tapped by lightning based on analysis of VHF emission density.

The National Lightning Detection Network (NLDN) provided CG flash data. The NLDN consists of a network of magnetic direction finder and time of arrival sensors used to locate in space and time ground strike locations of CG lightning. Information on CG polarity, peak current, and multiplicity also are available. The most recent NLDN upgrade, discussed in Cummins et al. (1998), gives greater than 90% detection efficiency and 0.5-km location accuracy within the STEPS domain.

The South Dakota School of Mines and Technology (SDSMT) armored T-28 aircraft provided in situ wind, microphysical, electric field, and particle charge data in the lower- to middle-altitude range within updrafts and hail shafts. The T-28 measured the complete spectrum of water and ice particles in clouds, ranging from cloud droplets a few micrometers in diameter to about 5-cm-diameter hail. One of its three precipitation particle imaging probes had the capability to determine particle charge as the particle is imaged (minimum sensitivity as low as 0.5 pC). In addition, it carried a six-instrument electric field meter system that maps the total vector electric field inside and outside clouds.

Mobile sounding systems from the National Oceanic and Atmospheric Administration/National Severe Storms Laboratory (NOAA/NSSL) obtained balloon-borne measurements of electric fields inside storms [electric field meter (EFM) balloons]. The main instrument was the balloon-borne EFM [originally developed by Winn and Byerley (1975)] that NSSL has improved and used for 15 yr. An overview of this instrument is provided by MacGorman and Rust (1998, their section 6.2.3). The electric field data yielded the full three-dimensional electric field vector and can be used to infer layers of net negative or positive charge (e.g., Stolzenburg and Marshall 1994). The mobile laboratory also contained standard surface meteorological sensors and a surface electric field meter.

NCAR mobile sounding systems [Mobile GPS/Loran Atmospheric Sounding System (M-GLASS)] and NOAA/NSSL mobile mesonet vehicles characterized the storm environment. The mesonet vehicles, which augment existing meteorological networks, consisted of meteorological instruments mounted on standard automobiles. They can provide accurate observations of pressure, temperature, and relative humidity, as well as wind direction and speed, whether the vehicle is moving or stationary. The M-GLASS systems were mounted on pickup trucks and made standard atmospheric sounding and surface measurements.

Finally, the Yucca Ridge Field Station (YRFS), located near Fort Collins, Colorado (275 km northwest of the LMA centroid; Fig. 1), provided observations of TLEs during STEPS. The YRFS, operated by FMA Research, made use of numerous on- and off-site instruments, including radio frequency (RF), telescopic, and photometric sensors along with low-light imagers. Data from up to six extremely low frequency (ELF) sensors on four different continents provided additional information on the parent lightning of TLE phenomena in the STEPS domain.

The combination of all of these observations provided, along with an understanding of each storm's mesoscale environment, a depiction of the coevolving kinematic, microphysical, and electrical structures and lightning behavior of STEPS thunderstorms. Because of the detailed observing network, the STEPS data provide a unique opportunity to answer key questions about precipitation formation and electrification within severe storms. Additionally, the presence of two polarimetric radars and in situ observations provided an opportunity to evaluate and improve radar-based hydrometeor identification and quantification algorithms.

The operations center for STEPS was at the CSU–CHILL radar facility, temporarily relocated from its home base at Greeley, Colorado, to Burlington, Colorado. Mobile facilities and STEPS personnel generally were based out of Burlington and Goodland, Kansas. STEPS received significant support from the local NWS forecast office in Goodland (see sidebar 1), and daily forecast and observational platform status briefings occurred each morning at this NWS facility.

Based on each briefing, we formulated operations plans for the afternoon and evening. The research radars (CSU–CHILL and S-Pol) typically were running surveillance scans by noon. When convection was likely, M-GLASS soundings were released at various locations and vehicle platforms (mobile mesonet, EFM balloons) were deployed in strategic locations where we expected activity. Once we identified convective targets, the vehicles and T-28 aircraft were vectored to the storm via two-way radio communications with the operations center. In addition, the research radars would begin synchronized sector-based plan position indicator (PPI) and RHI scans of the target storm.

The main focus of observations was storms that occurred within or passed through the dual-Doppler lobes formed by each radar pair within the STEPS network (see Fig. 1). Of these, the highest priority was supercell storms, especially those with LP characteristics, as well as thunderstorms observed to be producing predominantly +CGs.

EXAMPLES OF STEPS OBSERVATIONS.

Overview of STEPS cases. We were able to obtain data on a number of different cases during STEPS. Table 2 lists the major STEPS operations days, along with a short description of the most interesting storms of those days, and the most extreme severe storm reports (if any) associated with those storms. In addition, Table 2 lists the peak hourly percentage with positive polarity of all CGs that occurred within 125 km of the LMA network centroid. This is used as an indicator of positive CG production, as not all storms have had their lightning data (both NLDN and LMA) analyzed in detail yet. Only cases that had 10 or more CGs per hour at peak have percentages computed. Note that since STEPS instrumentation focused on storms producing the most +CGs, this column in Table 2 tends to underestimate the maximum percentage of +CGs in the target storm because of the potential inclusion of concurrent storms not producing as many +CGs. Despite this limitation, Table 2 demonstrates that most of the STEPS cases produced some sort of severe weather, and at least half were associated with more than 50% +CGs at peak (i.e., PPCG storms).

Indeed, it was the ubiquity of PPCG storms in this area that was one of the distinctive results of STEPS, in that the storms spanned vastly different organizational categories, from small isolated convection to various types of large multicell storms, as well as supercells. Both storms with LP characteristics (determined visually; total of three cases—31 May, 3 June, and 5 July) and non-LP storms exhibited this flash behavior. While most +CG storms were associated with severe weather, there was one PPCG case (6 June) that had no severe weather reports. In addition, there were examples of low-CG storms (less than

COOPERATION BETWEEN RESEARCH AND FORECAST COMMUNITIES

The NWS office in Goodland, Kansas was in a unique position to provide the STEPS experiment with logistical assistance, forecast personnel, local expertise, and volunteer field-team participants. Indeed, demonstration of cooperation between the forecast and research communities was a goal of the experiment. Preoperational phase support included assistance in facility procurement, sensor placement, climatological research, lodging assistance, and building local community support for the project. In addition, NWS personnel provided much of the local media support during STEPS, including arranging of the STEPS media day.

During the operational phase, the NWS office was the hub for planning and forecasting. Morning briefings occurred at the office through the use of both NWS computer resources and Web-based NCAR model output. NWS short-term forecasters and project investigators collaborated on forecast briefings. This allowed local expertise to be integrated into the operational decision process. Local NOAA Weather Radio stations disseminated a daily briefing summary.

Twenty-five volunteers from seven NWS offices participated in various support positions. The roles of these volunteers ranged from project nowcasters to field participants in the mobile mesonet and EFM ballooning operations. A two-way radio enhanced communications between the NWS office and the STEPS Operations Center (OC). NWS relayed fixed mesonet data, output from NWS analysis software [such as the Local Analysis and Prediction System (LAPS) and the System for Convection Analysis and Nowcasting (SCAN)], and severe weather reports to the OC during field operations.

The NWS benefited through exposure to unique datasets in near–real time. Forecaster access to M-GLASS soundings, timely reports from the mobile mesonet, and Web-based CSU–CHILL and NCAR S-Pol data all contributed to an improved warning program. Interaction with STEPS researchers, including seminars presented by project investigators, allowed NWS staff to increase their knowledge of convective processes and severe convection forecasting. The procedures and lessons learned during STEPS provided a model for NWS participation in the Bow Echo and Mesoscale Convective Vortex (MCV) Experiment (BAMEX) field project, which occurred in the summer of 2003.

Table 2. Overview of STEPS cases. Severity based on reports to NWS. Peak hourly positive CG percentage based on all CGs occurring during operations within 125 km of the LMA network centroid. N/A: Less than 10 CGs total in any 1 h.

Date	Storm summary	Peak severity	+CG peak hourly fraction
25 May	Convective line	No reports	7%
26 May	Convective line	0.75-in. hail	34%
31 May	Isolated LP storm	1-in. hail 70-kt gust	73%
3 Jun	Isolated LP storm	1-in. hail	N/A
6 Jun	Isolated storm	No reports	79%
9 Jun	Convective line	60-kt gust	37%
11 Jun	Asymmetric MCS	1.5-in. hail 57-kt gust	61%
12 Jun	Isolated storm	0.75-in. hail	N/A
19 Jun	Multicell storm	65-kt gust	10%
22 Jun	Convective line	F0 tornado 1.75-in. hail 60-kt gust	74%
23 Jun	Multicell storm	0.75-in. hail 60-kt gust	80%
24 Jun	Classic supercell	1-in. hail	96%
29 Jun	Classic supercell	F1 tornado 1.75-in. hail 61-kt gust	68%
1 Jul	Convective line	No reports	15%
5 Jul	LP supercell	Funnel cloud 1.75-in. hail 65-kt gust	93%
10 Jul	Multicell storm	1.75-in. hail 52-kt gust	75%
12 Jul	Isolated storm	No reports	28%
17 Jul	Convective line	No reports	37%
18 Jul	Convective line	1-in. hail 60-kt gust	28%
19 Jul	Convective line	F0 tornado 1.75-in. hail	88%
20 Jul	Convective line	Flash flood 1.75-in. hail 63-kt gust	88%

10 total CGs per hour at maximum) that had inverted polarity electrical structures, in that the main positive charge region appeared to lie within thunderstorm midlevels (i.e., near –20°C) and below the main negative charge region in contrast to what is most commonly seen in other storms (e.g., Stolzenburg et al.

a)

b)

Fig. 2. (a) Photograph of 29 Jun classic supercell taken at 2323 UTC, approximately 5 min before tornado touchdown. Photograph taken at S-Pol looking toward the ESE. Though taken too far away (60–70 km) to resolve the precipitation shaft, the cloud does not have the structure of an LP supercell like 5 Jul [shown in (b)]. Photo by C. Knight. (b) Photograph of the mature phase (after 2330 UTC) of the 5 Jul LP supercell. Notable visual characteristics are a striated, bell-shaped cloud that is often indicative of a rotating updraft, and very little precipitation to the north and east. Photo taken by M. Weisman from the SSE direction, approximately 5 miles from the updraft base.

1998a,b). The most prominent example was 3 June, a small isolated storm with LP characteristics that produced no CGs of either polarity but had a possibly inverted electrical structure based on inferences from an EFM balloon sounding and LMA intracloud flash behavior (Rust and MacGorman 2002; Hamlin et al. 2003). Many of the PPCG storms also appeared to have inverted polarity structures based on EFM and LMA data (Rust and MacGorman 2002; Hamlin et al. 2003; Rust et al. 2003). Apart from the main cases reviewed here, there were smaller storms with low total flash rates (2–3 min^{-1}) that exhibited inverted electrical behavior. One such storm, different from the supercell on that day, occurred on 24 June. An interesting contrast to these PPCG and potentially inverted storms is the severe multicell storm of 19 June, which produced at most 10% +CGs.

Based on Table 2, there are several case studies and comparisons that can be done to address the goals of the STEPS project. Many of these are either underway or planned. A main focus of STEPS was supercells, and the project obtained data on three. To illustrate how the STEPS suite of observing platforms worked together to accomplish project goals, we have selected two supercell cases for short overviews: a classic supercell that occurred on 29 June 2000, and an LP supercell that occurred on 5 July.

Overviews of the 29 June classic and 5 July LP supercells. Meteorological scenarios. The afternoon of 29 June 2000 saw an unstable air mass in western Kansas with sufficient shear for supercell-type storms. Surface dewpoints decreased toward the west into eastern Colorado, but a distinct dryline was not evident. A short line of convective cells developed around 2200 UTC in the northwest corner of Kansas. The convection subsequently moved southeastward, remaining in a multicellular phase for nearly 1.5 h before making a 35° right turn as it became more supercellular in character. The right turn is believed to be the result of gust front convergence favoring growth on the storm's right flank. Around this time, storm size increased dramatically and a tornado first touched ground (2328 UTC). The tornado was on the ground for about 16 min, and mobile mesonets tracked it throughout its lifetime. (A description and photogrammetric analysis of the tornado courtesy of E. Rasmussen is available online at www.nssl.noaa.gov/ssr/index.htm.) There also were multiple reports of large hail (up to 1.75 in. in diameter; Table 2), particularly after the midlife intensification and tornado touchdown. A photograph of the 29 June supercell taken near the time of the tornado is shown in Fig. 2a.

The weather scenario on 5 July was consistent with past conditions associated with LP supercell events, with a relatively quiescent synoptic environment and a strong dryline along the Kansas–Colorado border. CAPE and shear estimates east of the dryline supported a forecast for supercellular storms. In addition, an outflow boundary from a convective system earlier that morning in eastern Nebraska had propagated westward into southwestern Nebraska. The significant storm on this day subsequently developed to the northeast of this dryline–outflow intersection, within the highly unstable air mass, and quickly developed significant low and midlevel rotation and an

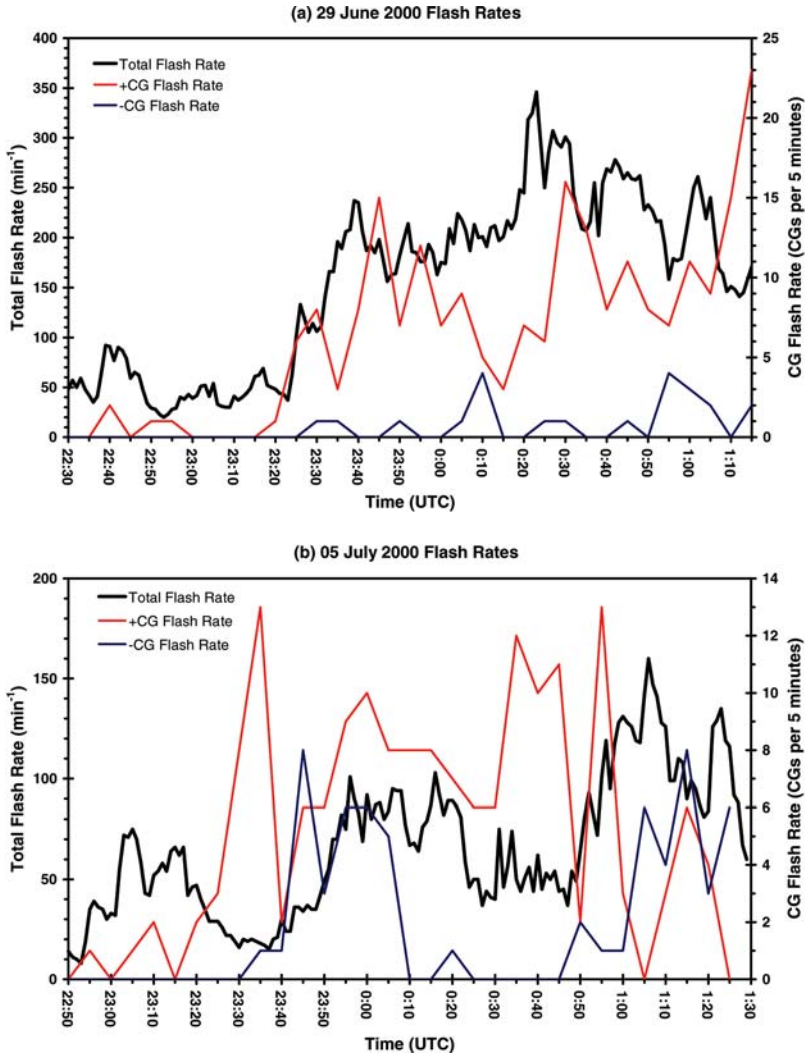

FIG. 3. (a) Time series of total and cloud-to-ground lightning flash rates for the 29 Jun 2000 classic supercell. (b) Same as (a), but for the 5 Jul 2000 low-precipitation supercell.

associated hook on the radar reflectivity field. A photo taken during its mature phase (after 2330 UTC; Fig. 2b) shows many of the characteristics of an LP supercell with a striated, bell-shaped cloud—often indicative of a rotating updraft—and visually very little precipitation just to the north and east of the primary cloud. This contrasts with the more amorphous cloud seen in the 29 June photo (Fig. 2a). This storm produced a funnel cloud at 0000 UTC (Table 2), along with some large hail (up to 1.75 in. in diameter).

LIGHTNING BEHAVIOR. We used the LMA and NLDN to characterize the lightning behavior of observed storms. Figure 3 shows total and CG lightning flash rate time series for the (a) 29 June and (b) 5 July supercells. Total flash rates were determined by the methodology described in Thomas et al. (2003), except that only flashes consisting of five or more VHF sources were included in order to minimize contamination by noise. NLDN data provided CG flash rates. Both storms featured very high total flash rates (> 1 flash per second) and were dominated by +CG lightning for much of their lifetimes. The supercells often underwent pulsations in total flash rate, and sometimes also +CG flash rates (Fig. 3). Perhaps the most notable of these pulses is the intensification of 29 June between 2320 and 2340 UTC. This is also the period when the storm underwent its right turn and produced a tornado.

Using polarimetric-based hydrometeor identification with CSU–CHILL and S-Pol data, we can estimate the volume of radar echo occupied by hail as a function of time and height. The hydrometeor classification algorithm used is fuzzy-logic based, developed from Liu and Chandrasekar (2000), Straka et al. (2000), and Zrnic et al. (2001). In addition, by manually isolating individual LMA flashes, we can determine the starting height of +CGs that occurred in the 29 June storm. The result of these efforts is shown in Fig. 4, which demonstrates that the increase in +CG production during 2320–2340 UTC was coincident with the presence of hail aloft. Additionally, the vast majority of positive CGs originated in the 0° to –20°C temperature range, which normally is where the main negative charge region is found in thunderstorms (Krehbiel 1986; Koshak and Krider 1989; Stolzenburg et al. 1998a,b).

A more direct link between hail aloft and the occurrence of +CG lightning is shown in Figs. 5 (29 June) and 6 (5 July), which show horizontal and vertical cross sections of LMA VHF sources associated with a single +CG flash from each storm, overlaid onto cross sections of radar reflectivity factor, multiple-Doppler-derived winds, and polarimetrically identified hail and graupel. These plots are typical of many +CGs in these storms, which tended to

initiate in or near regions of hail and high-density graupel aloft (initiation points are shown by white diamonds in Figs. 5 and 6), the latter being an intermediate category between regular graupel and small hail.

These strong updrafts often coincided with bounded weak echo regions (BWERs; Browning and Donaldson 1963; Browning 1964, 1965) in the reflectivity field, as well as "holes" in VHF sources detected by the LMA. Figure 7 shows an example of these phenomena from 29 June, with horizontal and vertical cross sections of LMA sources overlaid on contours of reflectivity factor and multiple-Doppler-derived updraft speeds. The lack of VHF sources is roughly collocated with the strong updraft in this storm (note that we did not wind-advect VHF sources like the radar data during multiple-Doppler synthesis, so given the high translational speed of this storm some mismatch is expected). The lack of VHF sources in strong updrafts has been observed before by Ray et al. (1987) and Krehbiel et al. (2000) and suggests lack of a vigorous process of charge separation in these regions.

Electric field observations. Information about the electric fields in thunderstorms is an important complement to LMA data, revealing information about the charge structure that would be otherwise unavailable from lightning data alone (e.g., Coleman et al. 2003). In particular, in situ measurements such as those from EFM balloons and T-28 storm penetrations can be used to reveal more clearly regions of net negative charge, since as mentioned previously the LMA is more sensitive to negative breakdown in regions of net positive charge (Rison et al. 1999). Electric field data also reveal charge layers not tapped by lightning discharges, or can confirm the lack of charge in parts of the storm untouched by lightning (such as the previously mentioned BWERs; e.g., Fig. 7).

We launched several EFM balloons into the 29 June and 5 July storms. To show how these soundings are being used to improve our understanding of electrical structure in STEPS storms, we compare updraft soundings from these 2 days. Figure 8 shows data from a 29 June updraft sounding, and Fig. 9 shows a corresponding sounding for 5 July. Inside the updrafts of both storms, electric field magnitudes remained small and fairly constant (typically < 10 kV m^{-1} in magnitude) until an altitude of ~8 km MSL, confirming the inference of little charge in strong updrafts based on LMA data (e.g., Fig. 7). In 29 June (Fig. 8), the electric field changed sign and indicated a positive charge layer between 8 and 10 km MSL (near –20°C) as the balloon entered regions of heavier precipitation, including hail (reflectivity > 50 dB*Z*). On 5 July (Fig. 9), however, the lowest charge region contained negative charge. But the next lowest charge region on 5 July, encountered at a height of 8.5 km MSL, did have positive charge comparable to the lowest positive charge on 29 June.

The charge distribution on 5 July also was similar to that on 29 June in that both storms had more complex charge structure during the descent in and near reflectivity cores than during the ascent through the strong updrafts, with charge extending to considerably lower altitudes in the reflectivity cores. Similar differences in the complexity of charge structure between strong updrafts and either weak updrafts or other portions of storms have been reported previously by Marshall et al. (1995) and Stolzenburg et al. (1998a,b; 2002).

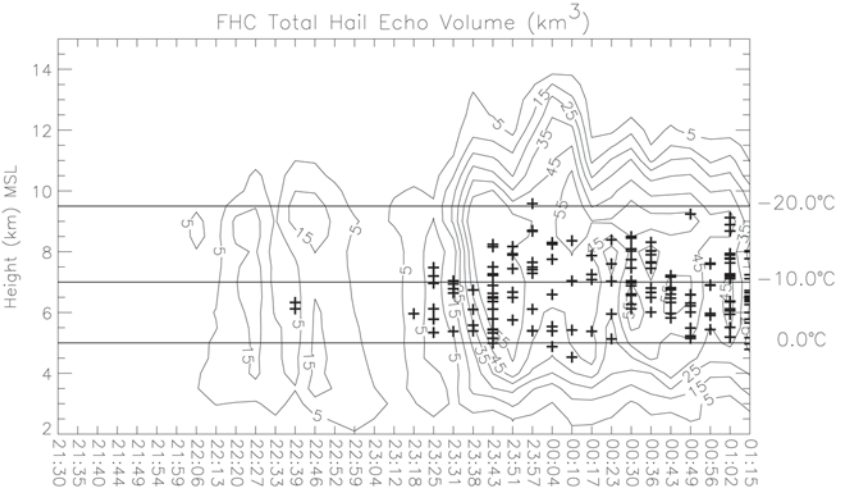

Fig. 4. Time–height cross section of 29 Jun 2000 hail echo volume (*not* radar reflectivity factor) as determined from both S-Pol and CHILL polarimetric data (radar used at each time is the one with the best coverage at that time) via a hydrometeor classification scheme using fuzzy logic techniques. Also shown are the starting heights for individual +CG flashes produced by the storm as determined by the LMA (black crosses), as well as notable temperature levels. The tornado occurred at 2328 UTC.

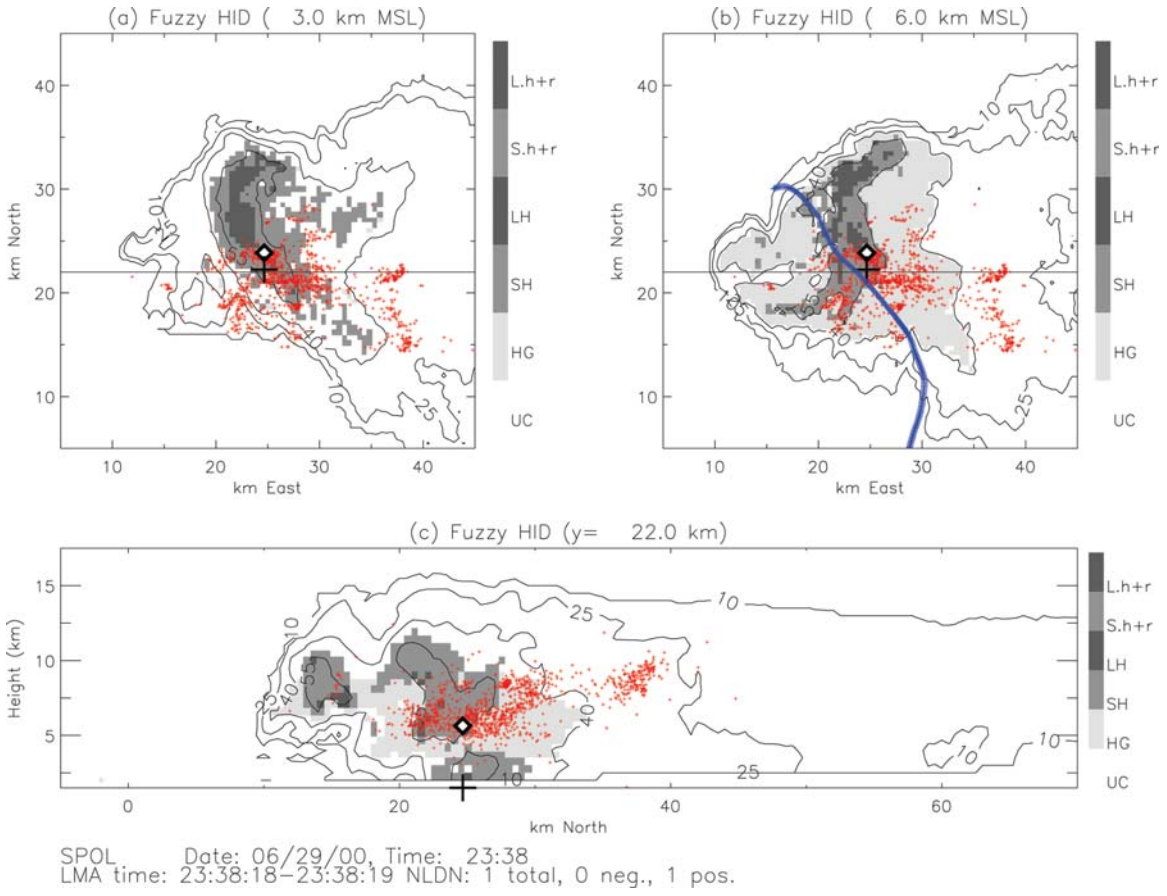

Fig. 5. (a) Horizontal cross section at 3 km MSL of hydrometeor identification (HID) categories (shaded), radar reflectivity factor (line contours, starting at 10 dBZ with 15 dBZ increments), and LMA VHF sources (red dots, sources from all altitudes projected onto the horizontal plane) associated with a +CG flash (strike location denoted by a black cross) that occurred at 2338:18 UTC on 29 Jun 2000. The location of the initial VHF source associated with the flash is indicated by the large white diamond with the black border. The only HID categories shaded are hail and high-density graupel related—large hail mixed with rain (Lh+r; hail diameter > 2 cm), small hail mixed with rain (Sh+r; D < 2 cm), large hail (LH), small hail (SH), and high-density graupel (HG). The polarimetric data are from an S-Pol PPI volume starting at 2338 UTC, and the line indicates the vertical cross section shown in (c). (b) Same as (a), but for 6 km MSL. The T-28 track for Fig. 10 is shown as the thick blue curve. (c) Vertical cross section of HID and radar reflectivity factor at 22 km north of the KGLD radar, along with LMA sources and +CG strike location projected onto the vertical plane. Legend is the same as in (a) and (b).

The T-28 made several passes through the main updraft region of the 29 June storm at the 6 km MSL (–10°C) level during the transition period when the storm produced a tornado and began producing frequent +CG lightning. The updraft and the electric field data from the last of these passes are shown in Fig. 10. The corresponding track is superimposed on the 6-km-horizontal cross section in Fig. 5 (aircraft was moving northward). Although the multiple-Doppler wind syntheses (Fig. 7) suggest a single extended updraft region around this time, the higher-resolution aircraft data show multiple discrete updrafts at 6 km. Consistent with the balloon EFM observations (Fig. 8), all except the southernmost updraft core were free of hail (weak radar echo) and were characterized by a weak negative vertical electric field (magnitude < 10 kV m^{-1}), suggesting relatively little net charge in the updrafts. Unfortunately, the T-28 was not available for the 5 July storm.

The T-28 provided the first in situ verification on an LMA-mapped flash channel during an earlier 29 June penetration (not shown in Fig. 10). During a pass across the downshear precipitation region, the T-28 encountered an intracloud lightning flash that was evident in both its electric field record and partially imaged by the wing-mounted video camera. The LMA also detected this flash. Warner et al. (2003) used the T-28 data to model the channel and estimate

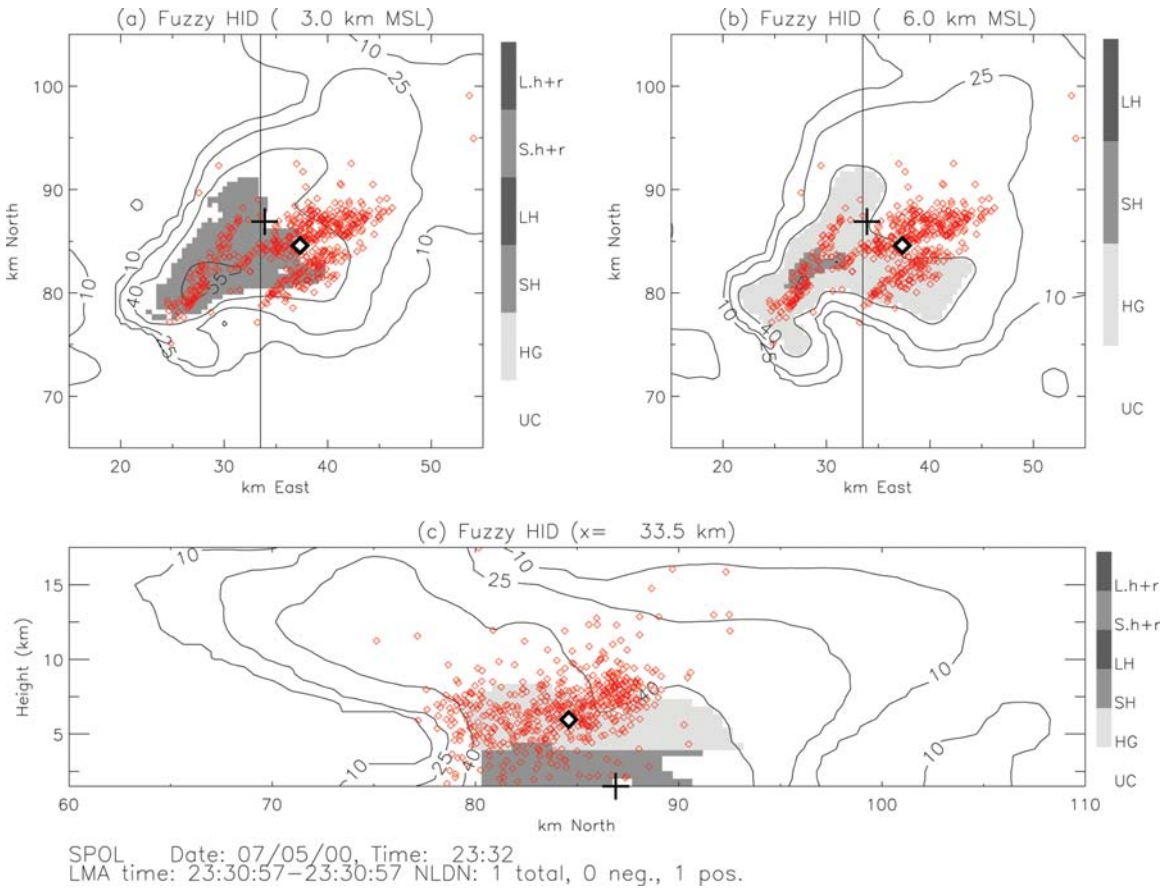

FIG. 6. Same as Fig. 5, but for the 2332 UTC S-Pol radar volume on 5 Jul 2000. The LMA points and CG strike location are for a +CG occurring at 2330:57 UTC. No T-28 track is shown.

its location, charge density, and polarity. The analysis agreed with the LMA-inferred polarity and channel orientation.

Thus, the electric field data not only help to confirm inferences of the lack of charge in strong updrafts in these storms, but also reveal complex charge structures outside these main updrafts that are not evident in the LMA data. In addition, the electric field data in concert with the LMA data show that both 29 June and 5 July had possibly inverted electrical structures, with midlevel (near –20°C) positive charge in place of midlevel negative charge. This inference is supported by preliminary modeling results for the 29 June storm by Kuhlman et al. (2003).These charge structures appear to be related to positive CG production. We continue to use STEPS data to investigate these charge structures in more detail, as well as to investigate exactly how they arose and to understand their relationship to positive CG production. These efforts include not just the supercells of 29 June and 5 July, but also other STEPS cases.

KINEMATIC AND MICROPHYSICAL STRUCTURES. Figure 11 shows the radar reflectivity factor and multiple-Doppler winds for the [(a),(b)] 29 June and [(c),(d)] 5 July supercells during their mature phases and demonstrates how similar the two supercells look to a radar, despite obvious differences in their visible cloud structures (Fig. 2). Both had strong updrafts in excess of 40 m s^{-1}, midlevel rotation, low-level hook echoes, BWERs in the vicinity of the updrafts, and high peak reflectivity factors (> 50 dB*Z*), although overall, 5 July had lower peak reflectivity than 29 June. One way to determine whether these gross radar-based similarities mask important microphysical differences is through the use of a numerical cloud model.

Such models have been successful at reproducing the basic dynamical character of the observed convective storm spectrum (e.g., ordinary cells, multicells, supercells, squall lines, etc.; Weisman and Klemp 1986; Weisman et al. 1988), but have been far less successful at reproducing the large variety of observed precipitation characteristics in any systematic

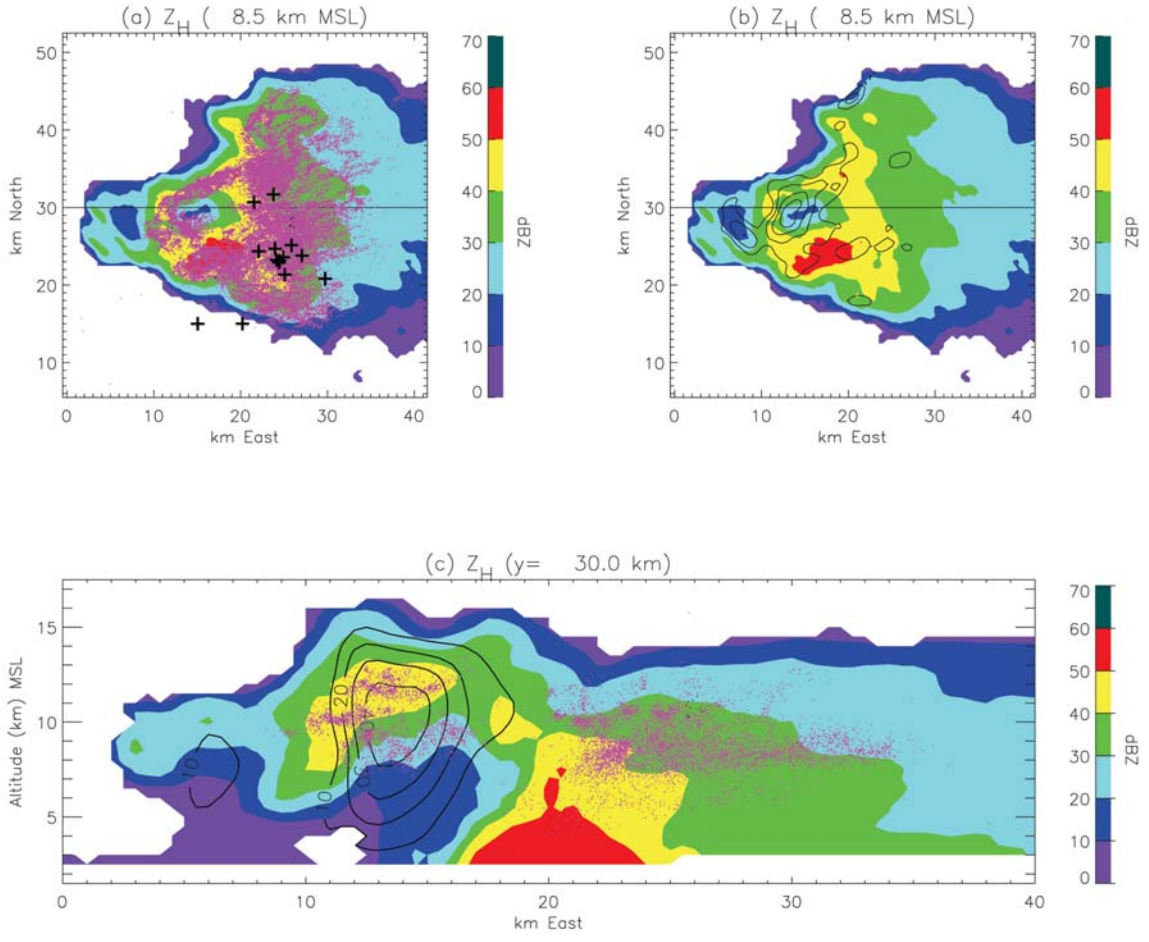

Fig. 7. (a) Horizontal cross section of radar reflectivity factor (synthesized from both CHILL and S-Pol; color contours) from 2325 UTC on 29 Jun 2000. Also shown are LMA-detected VHF source locations during 2325–2327 UTC and within 0.5 km of the cross-sectional cut (magenta dots), as well as NLDN-detected +CG ground strike locations during the radar volume (black crosses). LMA data have not been advection-corrected. (b) Same as (a), except lacking lightning data and instead showing updraft speeds (black contours; every 10 m s^{-1} starting at 10 m s^{-1}) as estimated by multiple-Doppler synthesis. (c) Vertical cross section at same time showing radar reflectivity, LMA-detected VHF source locations, and updraft speeds. Legend is the same as in (a) and (b).

or physically realistic manner (e.g., Weisman and Bluestein 1985). Additionally, numerical studies show great sensitivity in resultant convective structure, evolution, and precipitation output to relatively minor differences in microphysical schemes, casting much doubt on our current ability to forecast convective precipitation in operational models (e.g., Gilmore et al. 2003). Numerical modeling of storms observed in STEPS is an important goal of the project in order to improve our understanding of the precipitation processes in supercells and other storms. Observations from radar, the T-28, and soundings can be used to "teach" the model to come as close as possible (or as is practical) to the real storms. The model results then can be used as the basis for a detailed analysis of precipitation formation.

Some initial idealized simulations have been completed for both the 29 June and 5 July supercell storms using the Weather Research and Forecast model (WRF; http://wrf-model.org), with a 1-km (0.5 km) grid spacing in the horizontal (vertical) direction over a 120 km × 120 km × 22 km domain, and with the Lin et al. (1983) microphysics parameterizations, which includes six water species (water vapor, cloud water, cloud ice, snow, rain, and graupel; Miller and Weisman 2002). Preliminary results indicate that the model is able to replicate basic storm-scale properties, such as storm motion, orientation, and rotational characteristics, but these same model results also highlight the difficulties in reproducing the microphysical character of the storms. For instance, while both storms exhibited low-level hook echoes and vaulted radar struc-

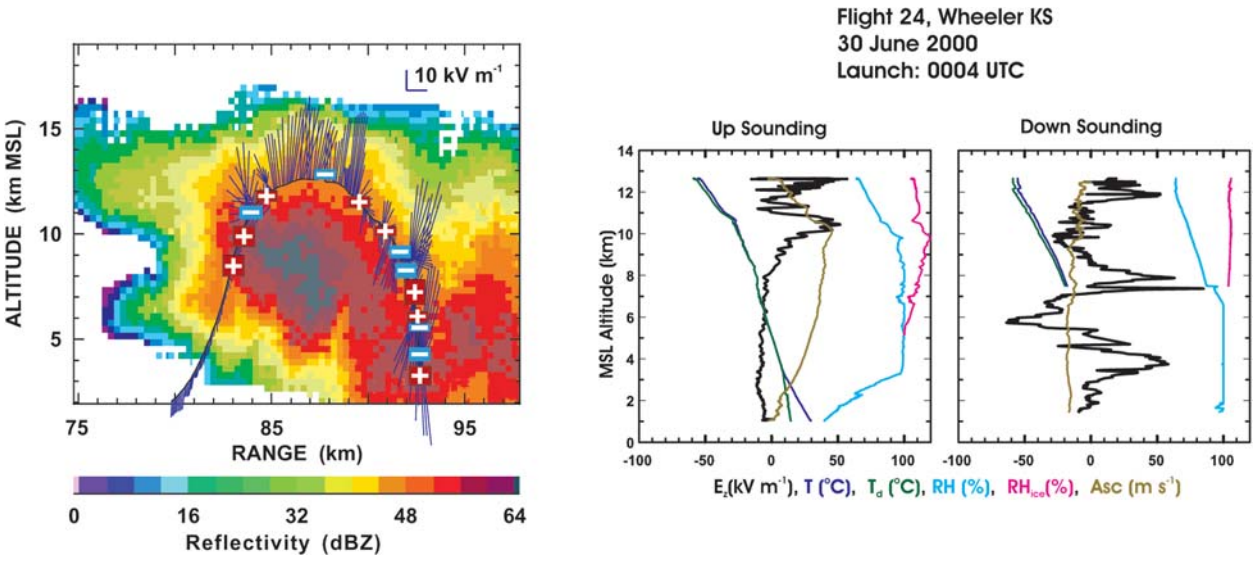

FIG. 8. Vertical cross section of reflectivity at an azimuth of 76° from the CSU–CHILL radar at 0010 UTC on 30 Jun 2000, shown with the projection of electric field vectors in this plane for the balloon flight during 0005–0034 UTC. Electric field vectors, shown in blue along the track (scale at the top), point from the balloon track along the direction a positive charge would move; the number of vectors has been reduced considerably for clarity in the figure. Red bars with plus signs show the vertical extent of positively charged regions inferred from the electric field profile (including all available vectors) and the lightning distribution, and blue bars with negative signs show the vertical extent of negatively charged regions. The balloon location has been corrected for storm motion to determine its path relative to storm structure at the time of the radar scan. The vertical component of electric field (E_z), temperature (T), dewpoint (T_d), ascent rate (Asc), and relative humidities (RH and RH_{ice}) are shown for the corresponding up and down soundings.

tures in the mid- to upper levels (Fig. 11), the simulations were not able to reproduce the vaulted structures. As the model updrafts (> 50 m s^{-1}) were comparable to observations, the fault appears to lie with the bulk microphysical parameterization used in the model, which requires that all like particles (e.g., graupel) fall with the same mean terminal velocity regardless of size. The simulations did produce a much weaker low-level cold pool for 5 July than it did for 29 June, which may be consistent with the 5 July storm's having a more LP-type structure, but this result was sensitive to changes in the microphysical parameters.

Future analyses will consider observations from

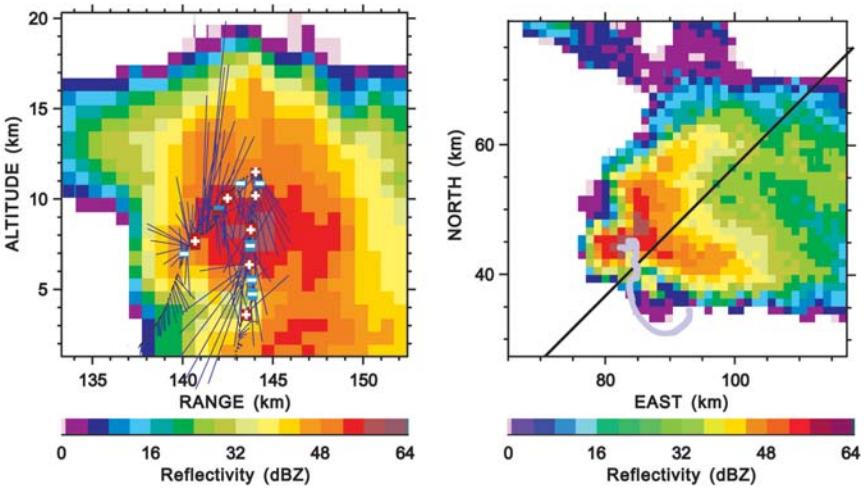

FIG. 9. Radar reflectivity, electric field, and inferred charge for the storm on 5 Jul 2000. (left) Vertical cross section of reflectivity at an azimuth of 45° from the CSU–CHILL radar at 0108 UTC on 6 Jul, shown with the projection of electric field vectors (electric field vector scale is the same as in Fig. 8) in this plane for the balloon flight during 0048–0127 UTC. The location of the balloon has been corrected for storm motion to show the storm-relative track at the time of the radar scan. Red bars with plus signs show the vertical extent of positively charged regions inferred from the electric field profile and the lightning distribution, and blue bars with negative signs show the vertical extent of negatively charged regions. (right) Storm-relative balloon track (black line) superimposed on reflectivity at an elevation of 0.5° from the NCAR S-Pol radar at 0119 UTC. The origin in each panel is the location of the radar that acquired the data.

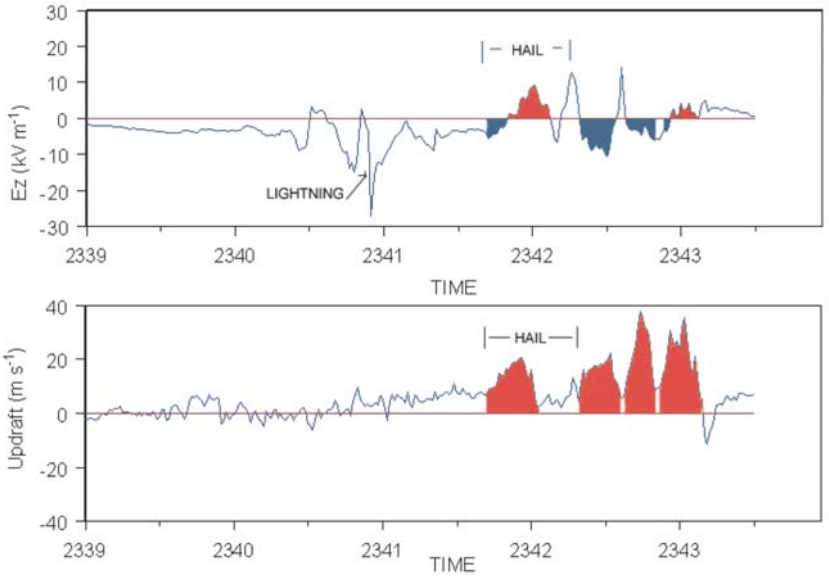

FIG. 10. Vertical component of the electric field and updraft are plotted vs time from the pass of the T-28 through the core of the storm between 2339:00 and 2343:30 UTC. (bottom) Four updraft cores are shaded in red. (top) The electric field magnitudes while the aircraft is in these cores are shaded red when positive and blue when negative. In the first southeasternmost updraft there is hail and positive field, while in the remaining three cores, the last two of which are precipitation free, the field tends to be negative. Field magnitudes are always less than 10 kV m^{-1}. An abrupt field change due to nearby lightning is noted just before 2341:00 UTC. "Hail" indicates when hail was observed by the T-28 microphysical sensors.

the T-28 aircraft and inferences from the polarimetric radar measurements to improve both the microphysical parameterization schemes and (hopefully) the simulated storm representations, especially cold-pool production and distribution of precipitation relative to the updraft. In addition, we plan to examine how the surrounding environment affects the kinematic and microphysical structures of LP storms. However, because the main differences between LP and other storms are likely to be microphysical, a key remaining challenge in modeling LP storms is accurate representation of the microphysics.

TLE observations. Within High Plains convection, sprites typically accompany only a small percentage of +CG flashes, most often within the stratiform precipitation region of larger MCSs (Lyons 1996). Sprites appear to represent conventional dielectric breakdown in themesosphere (~70–75 km MSL) triggered by unusually large electric field transients from +CGs below. Huang et al. (1999) noted that the key metrics in sprite formation should be the magnitude of the CG lightning vertical charge moment (M_q), the product of charge lowered to ground by a CG flash (C), and the height from which this occurs (Z_q).

STEPS documented more than 1200 TLEs, mostly sprites (Lyons et al. 2003a,b). Because STEPS featured a lightning mapper (the LMA) in close proximity to the Yucca Ridge Field Station, which recorded observations of TLEs, it provided an opportunity to distinguish sprite-parent +CGs (SP+CGs) from other lightning flashes. During STEPS, a half-dozen remote locations coordinated measurements of ELF transient signatures, allowing for both global-scale geolocation (Price et al. 2002) and estimates of M_q of the SP+CGs (Hu et al. 2002). LMA mapping of SP+CGs provided the height of the charge layers tapped by the CG strokes (Z_q; Lyons et al. 2003b). Data from STEPS show that SP+CG flashes are associated with both very high M_q values (>1000 C km for 90% probability of sprites) and low-altitude Z_q values (~4 km AGL; Hu et al. 2002; Lyons et al. 2003b). These results support the conceptual models of Williams (1998) and Huang et al. (1999), suggesting that the charge reservoir for SP+CGs would be found within the lower portions of MCS stratiform regions and are consistent with past measurements of positive charge layer height in MCSs (e.g., Schuur et al. 1991; Stolzenburg et al. 1994; Marshall et al. 2001).

STEPS OUTREACH AND EDUCATION. Outreach to the general public was a key component of STEPS. We scheduled a media day for the project that helped increase exposure to the general public. Several reports on STEPS occurred in the national and international media. Locally, there were news broadcasts on network-affiliate television stations in Colorado and Kansas and stories in major regional newspapers.

Local community outreach efforts were organized by the Colorado Climate Center at Colorado State University, in concert with an extension of the Community Collaborative Rain and Hail Study (CoCoRaHS; www.cocorahs.org), which uses local volunteer observers to report rain and hail measurements. These efforts involved cooperation with local

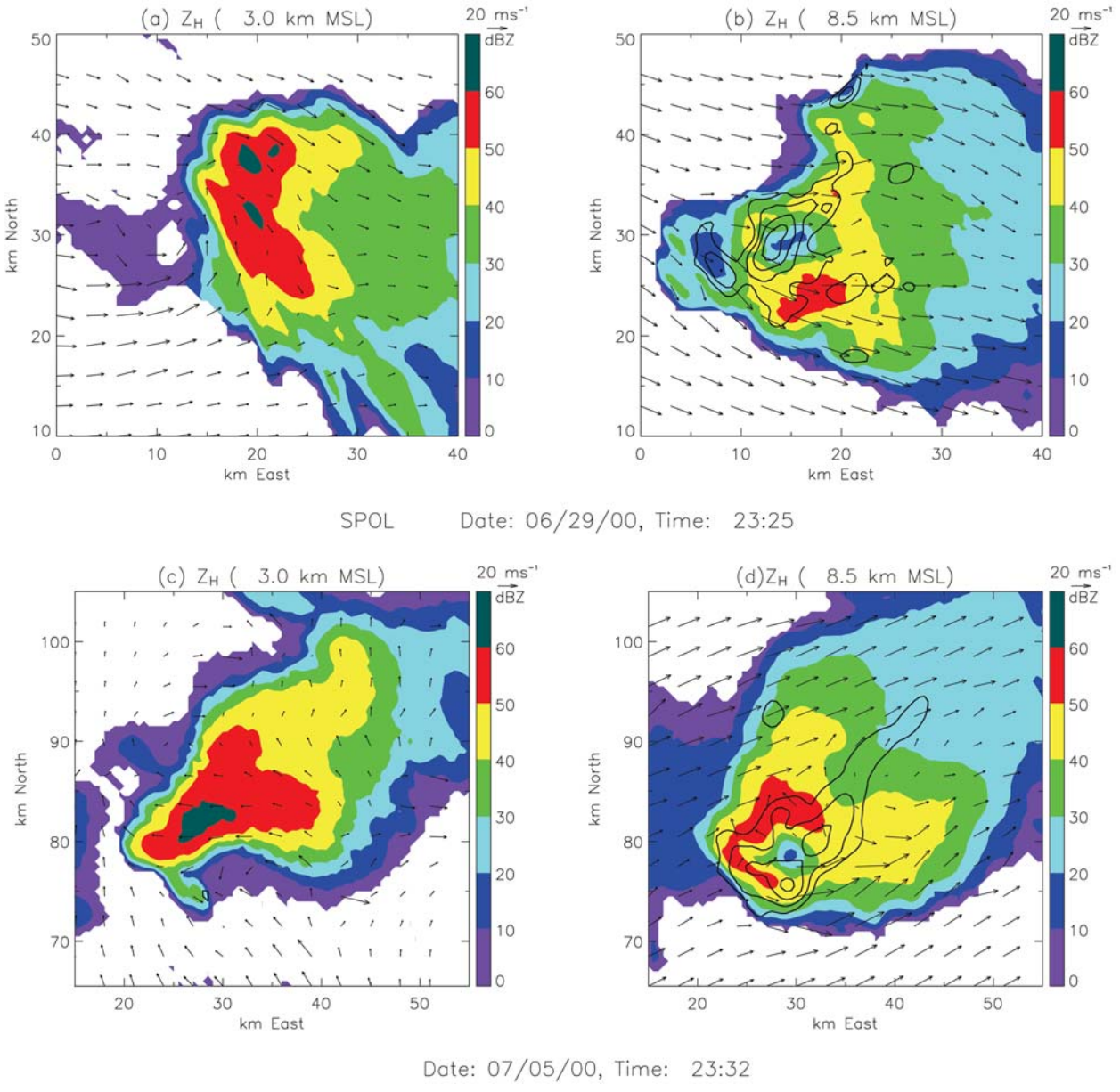

FIG. 11. (a) Horizontal cross section at 3 km MSL of radar reflectivity factor (from S-Pol; color shaded), multiple-Doppler wind vectors, and in (b) and (d) updraft speeds (line contours; every 10 m s^{-1} starting at 10 m s^{-1}) for the 29 Jun storm at 2325 UTC. (b) Same as (a), but for 8.5 km MSL. (c) Same as (a), but for 2332 UTC on 5 Jul. (d) Same as (c) but for 8.5 km MSL.

schools, whose students manufactured equipment for deploying hail pads, which the volunteers used to measure the number, size, shape, and density of hailstones. STEPS investigators also visited local schools and gave presentations on the project to interested members of the community.

STEPS provided research exposure to many undergraduate and graduate students. Besides the participation of students of STEPS investigators, a National Science Foundation (NSF)-funded Research Experience for Undergraduates (REU) program was conducted. In addition, the Significant Opportunities in Atmospheric Research (SOARS; www.ucar.edu/soars) program—cosponsored by the University Corporation for Atmospheric Research (UCAR), NSF, the U.S. Department of Energy (DOE), the National Aeronautics and Space Administration (NASA), and NOAA—provided the opportunity for students to work during the field campaign and do STEPS-related research afterward.

Finally, support from the NSF Informal Science Education program allowed production of a plan-

etarium program and home/classroom video, *The Hundred Year Hunt for the Red Sprite,* featuring the role of STEPS research in determining the atypical nature of the sprite-parent lightning discharges (see www.Sky-Fire.TV for details).

CONCLUDING REMARKS. The STEPS project has provided the research community with observations of the evolving kinematic, microphysical, and electrical structures of a diverse array of thunderstorms, including the primary targets of the experiment: supercells and predominantly positive CG (PPCG) storms. The project also provided both polarimetric and in situ microphysical data to help improve polarimetric radar–based hydrometeor classification and quantification schemes, as well as an opportunity to study the reasons transient luminous events (TLEs) occur above thunderstorms.

The cooperation between the NWS and atmospheric research communities, as well as outreach to the general public, were major goals of STEPS. These two activities are increasingly identified as major factors in a field project's overall success (e.g., Schultz et al. 2002), and the efforts to maximize outreach and intercommunity cooperation during STEPS could help provide a model for future field projects.

The combination of polarimetric and multiple-Doppler radar observations, along with LMA-based lightning mapping and in situ observations of electric field structure, may provide new insights into the nature of predominantly +CG thunderstorms. For example, comparisons of the 29 June and 5 July supercells suggest important linkages between strong updrafts, the development of large hail aloft, anomalous charging in thunderstorm midlevels, and subsequent production of positive CG flashes. These potential interrelationships between thunderstorm kinematics, microphysics, electrical structure, and lightning are the subject of ongoing research, not only in the aforementioned supercells but also other STEPS storms.

Indeed, a key to unlocking the mystery of PPCG thunderstorms, as well as other storms with inverted-polarity charge structures, could be identifying and understanding the common kinematic, microphysical, and electrical features of all such thunderstorms observed in STEPS. In addition, we need to understand the key differences between these storms and storms like that on 19 June 2000, which was severe but produced mostly –CGs Because all of these storms spanned different mesoscale environments, organizational structures, and levels of severity, this is a major research task that is still ongoing. Look for more STEPS results in both current and future publications.

ACKNOWLEDGMENTS. The STEPS project was funded by the National Science Foundation through the Physical Meteorology, Aeronomy, and Lower Atmospheric Observing Facilities programs. In particular, STEPS would not have occurred without the support and guidance provided by Dr. Rod Rogers at NSF/ATM. NSF also funded the REU component of STEPS. NOAA and the National Center for Atmospheric Research provided significant support for STEPS as well. In addition, the extensive collaboration with the National Weather Service, in particular the Goodland office, was a major key to the project's success. The STEPS community appreciates the great cooperation of the governments, schools, and general public of the cities of Burlington, Colorado, and Goodland, Kansas. Ken Cummins and Global Atmospherics, Inc., now part of Vaisala, generously provided the NLDN lightning data. Data collection, as well as installation and teardown of major facilities like the CSU–CHILL and S-Pol radars, was primarily the result of the dedicated staffs of all of the instrument platforms, as well as the tremendous number of enthusiastic undergraduate and graduate students who participated in the field campaign. People who made extraordinary contributions to STEPS data collection and analysis include Eric Bruning, Larry Carey, Tim Hamlin, Jeremiah Harlin, Sang-Hun Lim, Thomas E. Nelson, Walt Petersen, Sarah Tessendorf, and Kyle Wiens. We thank Bruce Entwistle at the Goodland NWS office for providing additional severe storm reports not available in *Storm Data.* Steve Nesbitt provided last-minute assistance with some figures in this paper.

REFERENCES

Bluestein, H. B., and C. R. Parks, 1983: A synoptic and photographic climatology of low-precipitation severe thunderstorms in the southern plains. *Mon. Wea. Rev.,* **111,** 2034–2046.

——, and G. R. Woodall, 1990: Doppler-radar analysis of a low-precipitation severe storm. *Mon. Wea. Rev.,* **118,** 1640–1664.

Branick, M. L., and C. A. Doswell III, 1992: An observation of the relationship between supercell structure and lightning ground strike polarity. *Wea. Forecasting,* **7,** 143–149.

Browning, K. A., 1964: Airflow and precipitation trajectories within severe local storms which travel to the right of the winds. *J. Atmos. Sci.,* **21,** 634–639.

——, 1965: Some inferences about the updraft within a severe local storm. *J. Atmos. Sci.,* **22,** 669–677.

——, and R. J. Donaldson, 1963: Airflow and structure of a tornadic storm. *J. Atmos. Sci.,* **20,** 533–545.

Burgess, D. W., and R. P. Davies-Jones, 1979: Unusual tornadic storms in eastern Oklahoma on 5 December 1975. *Mon. Wea. Rev.,* **107,** 451–457.

Carey, L. D., and S. A. Rutledge, 1998: Electrical and multiparameter radar observations of a severe hailstorm. *J. Geophys. Res.,* **103,** 13 979–14 000.

——, and ——, 2003: Characteristics of cloud-to-ground lightning in severe and nonsevere storms over the central United States from 1989–1998. *J. Geophys. Res.,* **108,** 4483, doi:10.1029/2002JD002951.

——, ——, and W. A. Petersen, 2003: The relationship between severe storm reports and cloud-to-ground lightning polarity in the contiguous United States from 1989 to 1998. *Mon. Wea. Rev.,* **131,** 1211–1228.

Changnon, S. A., Jr., 1977: The climatology of hail in North America. *Hail: A Review of Hail Science and Hail Suppression*, *Meteor. Monogr.* No. 38, Amer. Meteor. Soc., 107–128.

Coleman, L. M., T. C. Marshall, M. Stolzenburg, T. Hamlin, P. Krehbiel, W. Rison, and R. J. Thomas, 2003: Effects of charge and electrostatic potential on lightning propagation. *J. Geophys. Res.,* **108,** 4298, doi:10.1029/2002JD002718.

Cummins, K. L., M. J. Murphy, E. A. Bardo, W. L. Hiscox, R. B. Pyle, and A. E. Pifer, 1998: A combined TOA/MDF technology upgrade of the U.S. National Lightning Detection Network. *J. Geophys. Res.,* **103,** 9035–9044.

Curran, E. B., and W. D. Rust, 1992: Positive ground flashes produced by low-precipitation thunderstorms in Oklahoma on 26 April 1984. *Mon. Wea. Rev.,* **120,** 544–553.

Davies-Jones, R. P., D. W. Burgess, and L. R. Lemon, 1976: An atypical tornado producing cumulonimbus. *Weather,* **31,** 336–347.

Donaldson, R., A. Spatola, and K. Browning, 1965: Visual observations of severe weather phenomena. A family outbreak of severe local storms—A comprensive study of the storms in Oklahoma on 26 May 1963. Part I. Special Rep. 32, Air Force Cambridge Research Laboratory, 73–97.

Doswell, C. A., III, and D. W. Burgess, 1993: Tornadoes and tornadic storms: A review of conceptual models. *The Tornado: Its Structure, Dynamics, Prediction, and Hazards, Geophys. Monogr.,* No. 79, Amer. Geophys. Union, 161–172.

Gilmore, M. S., J. M. Straka, and E. N. Rasmussen, 2003: Precipitation and evolution sensitivity in simulated deep convective storms: Comparisons between liquid-only and simple ice and liquid phase microphysics. *Mon. Wea. Rev.,* in press.

Hamlin, T., P. R. Krehbiel, R. J. Thomas, W. Rison, and J. Harlin, 2003: Electrical structures and storm severity inferred by 3-D lightning mapping observations during STEPS. *Proc. 12th Int. Conf. on Atmospheric Electricity,* Versailles, France, International Commission on Atmospheric Electricity, 189–192.

Hu, W., S. Cummer, W. A. Lyons, and T. E. Nelson, 2002: Lightning charge moment changes for the initiation of sprites. *Geophys. Res. Lett.,* **29,** 1279, doi:10.1029/2001GL014593.

Huang, E., E. R. Williams, R. Boldi, S. Heckman, W. A. Lyons, M. Taylor, T. E. Nelson, and C. Wong, 1999: Criteria for sprites and elves based on Schumann resonance observations. *J. Geophys. Res.,* **104,** 16 943–16 964.

Klemp, J. B., 1987: Dynamics of tornadic thunderstorms. *Ann. Rev. Fluid Mech.,* **19,** 369–402.

Koshak, W. J., and E. P. Krider, 1989: Analysis of lightning field changes during active Florida thunderstorms. *J. Geophys. Res.,* **94,** 1165–1186.

Krehbiel, P. R., 1986: The electrical structure of thunderstorms. *The Earth's Electrical Environment,* E. P. Krider and R. G. Roble, Eds., National Academy Press, 90–113.

——, R. J. Thomas, W. Rison, T. Hamlin, J. Harlin, and M. Davis, 2000: GPS-based mapping system reveals lightning inside storms. *Eos, Trans. Amer. Geophys. Union,* **81,** 21–25.

Kuhlman, K. M., E. R. Mansell, C. L. Ziegler, D. R. MacGorman, and J. M. Straka, 2003: Charging and lightning in simulations of the 29 June 2000 STEPS supercell. *Proc. 12th Int. Conf. on Atmospheric Electricity,* Versailles, France, International Commission on Atmospheric Electricity, 199–202.

Lin, Y.-L., R. D. Farley, and H. D. Orville, 1983: Bulk parameterization of the snow field in a cloud model. *J. Climate Appl. Meteor.,* **22,** 1065–1092.

Liu, H., and V. Chandrasekar, 2000: Classification of hydrometeors based on polarimetric radar measurements: Development of fuzzy logic and neuro-fuzzy systems, and in situ verification. *J. Atmos. Oceanic Technol.,* **17,** 140–164.

Lyons, W. A., 1996: Sprite observations above the U.S. High Plains in relation to their parent thunderstorm systems. *J. Geophys. Res.,* **101,** 29 641–29 652.

——, R. A. Armstrong, E. R. Williams, and E. A. Bering, 2000: The hundred year hunt for the sprite. *Eos, Trans. Amer. Geophys. Union,* **81,** 373–377.

——, T. E. Nelson, R. A. Armstrong, V. P. Pasko, and M. A. Stanley, 2003a: Upward electrical discharges from thunderstorm tops. *Bull. Amer. Meteor. Soc.,* **84,** 445–454.

——, ——, E. R. Williams, S. A. Cummer, and M. A. Stanley, 2003b: Characteristics of sprite-producing positive cloud-to-ground lightning during the 19 July 2000 STEPS mesoscale convective systems. *Mon. Wea. Rev.,* **131,** 2417–2427.

MacGorman, D. R., and W. D. Rust, 1998: *The Electrical Nature of Storms*. Oxford University Press, 422 pp.

Marshall, T. C., W. D. Rust, and M. Stolzenburg, 1995: Electrical structure and updraft speeds in thunderstorms over the southern Great Plains. *J. Geophys. Res.,* **100,** 1001–1015.

——, M. Stolzenburg, W. D. Rust, E. R. Williams, and R. Boldi, 2001: Positive charge in the stratiform cloud of a mesoscale convective system. *J. Geophys. Res.,* **106,** 1157–1163.

Mazur, V., E. Williams, R. Boldi, L. Maier, and D. E. Proctor, 1997: Initial comparison of lightning mapping with operational time-of-arrival and interferometric systems. *J. Geophys. Res.,* **102,** 11 071–11 085.

Miller, L. J., and M. Weisman, 2002: Comparison of radar-observed and WRF-modeled structures of two STEPS storms. *Proc., 21st Conf. on Severe Local Storms,* San Antonio, Texas, Amer. Meteor. Soc., 299–302.

Orville, R. E., 1994: Cloud-to-ground lightning flash characteristics in the contiguous United States: 1989–1991. *J. Geophys. Res.,* **99,** 10 833–10 841.

——, and A. C. Silver, 1997: Lightning ground flash density in the contiguous United States: 1992–1995. *Mon. Wea. Rev.,* **125,** 631–638.

——, and G. R. Huffines, 2001: Cloud-to-ground lightning in the United States: NLDN results in the first decade, 1989–1998. *Mon. Wea. Rev.,* **129,** 1179–1193.

Price, C., M. Asfur, W. Lyons, and T. Nelson, 2002: An Improved ELF/VLF method for globally geolocating sprite-producing lightning. *Geophys. Res. Lett.,* **29,** 1031, doi:10.1029/2001GL013519.

Rasmussen, E. N., and J. M. Straka, 1998: Variations in supercell morphology. Part I: Observations of the role of upper-level storm-relative flow. *Mon. Wea. Rev.,* **126,** 2406–2421.

Ray, P. S., D. R. MacGorman, W. D. Rust, W. L. Taylor, and L. W. Rasmussen, 1987: Lightning location relative to storm structure in a supercell storm and a multicell storm. *J. Geophys. Res.,* **92,** 5713–5724.

Rison, W., R. J. Thomas, P. R. Krehbiel, T. Hamlin, and J. Harlin, 1999: A GPS-based three-dimensional lightning mapping system: Initial observations in New Mexico. *Geophys. Res. Lett.,* **26,** 3573–3576.

Rust, W. D., and D. R. MacGorman, 2002: Possibly inverted-polarity electrical structures in thunderstorms during STEPS. *Geophys. Res. Lett.,* **29,** 1571, doi:10.1029/2001GL014303.

——, ——, P. R. Krehbiel, R. J. Thomas, E. C. Bruning, and S. A. Stroman, 2003: The status of our search for inverted polarity electrical structures in thunderstorms. *Proc. 12th Int. Conf. on Atmospheric Electricity,* Versailles, France, International Commission on Atmospheric Electricity, 135–138.

Schultz, D. M., and Coauthors, 2002: Understanding Utah winter storms: The Intermountain Precipitation Experiment. *Bull. Amer. Meteor. Soc.,* **83,** 189–210.

Schuur, T. J., B. F. Smull, W. D. Rust, and T. C. Marshall, 1991: Electrical and kinematic structure of the stratiform precipitation region trailing an Oklahoma squall line. *J. Atmos. Sci.,* **48,** 825–842.

Stolzenburg, M., and T. C. Marshall, 1994: Testing models of thunderstorm charge distributions with Coulomb's law. *J. Geophys. Res.,* **99,** 25 921–25 932.

——, ——, W. D. Rust, and B. F. Smull, 1994: Horizontal distribution of electrical and meteorological conditions across the stratiform region of a mesoscale convective system. *Mon. Wea. Rev.,* **122,** 1777–1797.

——, W. D. Rust, and T. C. Marshall, 1998a: Electrical structure in thunderstorm convective regions. Part II: Isolated storms. *J. Geophys. Res.,* **103,** 14 079–14 096.

——, ——, and ——, 1998b: Electrical structure in thunderstorm convective regions. Part III: Synthesis. *J. Geophys. Res.,* **103,** 14 097–14 108.

——, T. C. Marshall, W. D. Rust, and D. L. Bartels, 2002: Two simultaneous charge structures in thunderstorm convection. *J. Geophys. Res.,* **107,** 4352, doi:10.1029/2001JD000904.

Straka, J. M., D. S. Zrnic, and A. V. Ryzhkov, 2000: Bulk hydrometeor classification and quantification using polarimetric radar data: Synthesis of relations. *J. Appl. Meteor.,* **39,** 1341–1372.

Thomas, R., P. Krehbiel, W. Rison, J. Harlin, T. Hamlin, and N. Campbell, 2003: The LMA flash algorithm. *Proc. 12th Int. Conf. on Atmospheric Electricity,* Versailles, France, International Commission on Atmospheric Electricity, 655–656.

Vivekandan, J., S. M. Ellis, R. Oye, D. S. Zrnic, A. V. Ryzhkov, and J. Strata, 1999: Cloud microphysics retrieval using S-band dual-polarization radar measurements. *Bull. Amer. Meteor. Soc.,* **80,** 381–388.

Warner, T. A., J. H. Helsdon Jr., and A. G. Detwiler, 2003: Aircraft observations of a lightning channel in STEPS. *Geophys. Res. Lett.,* **30,** 1984, doi:10.1029/2003GL017334.

Weisman, M. L., and H. B. Bluestein, 1985: Dynamics of numerically simulated LP storms. Preprints, *15th Conf. on Severe Local Storms,* Indianapolis, IN, Amer. Meteor. Soc., 167–171.

——, and J. B. Klemp, 1986: Characteristics of isolated convective storms. *Mesoscale Meteorology and Forecasting,* P. Ray, Ed., Amer. Meteor. Soc., 331–357.

——, and L. J. Miller, 2000: An overview of the severe thunderstorm electrification and precipitation study (STEPS). Preprints, *20th Conf. on Severe Local Storms,* Orlando, FL, Amer. Meteor. Soc., 273–276.

——, ——, and R. Rotunno, 1988: The structure and evolution of numerically simulated squall lines. *J. Atmos. Sci.,* **45,** 1990–2013.

Williams, E. R., 1989: The tripole structure of thunderstorms. *J. Geophys. Res.,* **94,** 13 151–13 167.

——, 1998: The positive charge reservoir for sprite-producing lightning. *J. Atmos. Sol. Terr. Phys.,* **60,** 689–692.

——, 2001: The electrification of severe storms. *Severe Convective Storms,* Meteor. Monogr. No. 49, Amer. Meteor. Soc., 527–561.

Winn, W. P., and L. G. Byerley III, 1975: Electric field growth in thunderclouds. *Quart. J. Roy. Meteor. Soc.,* **101,** 979–994.

Zajac, B. A., and S. A. Rutledge, 2001: Cloud-to-ground lightning activity in the contiguous United States from 1995 to 1999. *Mon. Wea. Rev.,* **129,** 999–1019.

Zrnic, D. S., A. Ryzhkov, J. Straka, Y. Liu, and J. Vivekandan, 2001: Testing a procedure for automatic classification of hydrometeor types. *J. Atmos. Oceanic Technol.,* **18,** 892–913.